ALD Al$_2$O$_3$-Coated TiO$_2$ Nanotube Layers as Anodes for Lithium-Ion Batteries

Hanna Sopha,[†] Girish D. Salian,[‡] Raul Zazpe,[†] Jan Prikryl,[†] Ludek Hromadko,[†] Thierry Djenizian,*[,§] and Jan M. Macak*[,†]

[†]Center of Materials and Nanotechnologies, Faculty of Chemical Technology, University of Pardubice, Nam. Cs. Legii 565, 53002 Pardubice, Czech Republic

[‡]Aix Marseille Université, CNRS, Electrochemistry of Materials Research Group, MADIREL UMR 7246, F-13397 Marseille Cedex 20, France

[§]IMT Mines Saint-Etienne, Center of Microelectronics in Provence, Department of Flexible Electronics, F-13541 Gardanne, France

S *Supporting Information*

ABSTRACT: The utilization of the anodic TiO$_2$ nanotube layers, with uniform Al$_2$O$_3$ coatings of different thicknesses (prepared by atomic layer deposition, ALD), as the new electrode material for lithium-ion batteries (LIBs), is reported herein. Electrodes with very thin Al$_2$O$_3$ coatings (~1 nm) show a superior electrochemical performance for use in LIBs compared to that of the uncoated TiO$_2$ nanotube layers. A more than 2 times higher areal capacity is received on these coated TiO$_2$ nanotube layers (~75 vs 200 μAh/cm^2) as well as higher rate capability and coulombic efficiency of the charging and discharging reactions. Reasons for this can be attributed to an increased mechanical stability of the TiO$_2$ nanotube layers upon Al$_2$O$_3$ coating, as well as to an enhanced diffusion of the Li$^+$ ions within the coated nanotube layers. In contrast, thicker ALD Al$_2$O$_3$ coatings result in a blocking of the electrode surface and therefore an areal capacity decrease.
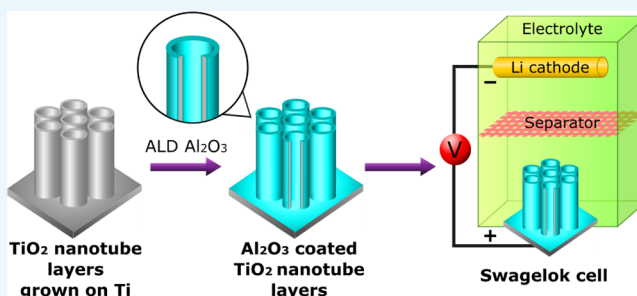
■ INTRODUCTION

During the last decade, TiO$_2$ nanomaterials have widely been studied as an alternative electrode material for lithium-ion batteries (LIBs).[1−15] TiO$_2$ has a higher lithiation potential (~1.6 V vs Li/Li$^+$) compared to that of the negative electrodes, such as graphite (~0.1 V vs Li/Li$^+$), and therefore enhances safety of the cells and provides a good capacity retention on cycling and a low self-discharge.[1−4] Furthermore, TiO$_2$ shows low volume changes of less than 4% upon reversible insertion and extraction of Li$^+$ in the lattice. However, TiO$_2$ also has a poor electrical conductivity and shows limited Li$^+$ uptake and slow Li$^+$ insertion kinetics.[1−4] To overcome these drawbacks, nanostructured TiO$_2$, such as mesoporous microspheres,[5] nanowires,[6,7] nanoparticles,[8] nanoflakes,[9] or TiO$_2$ nanotubes,[1−4,10] produced via different methods have been considered as anodes due to the larger specific surface area. Although most of these structures are randomly oriented and have to be deposited on the back contact of the electrode, self-organized TiO$_2$ nanotube layers produced by electrochemical anodization of the Ti substrates consist of straight and vertically aligned nanotubes in direct electrical contact with the underlying Ti substrate.[16] Another advantage of the vertically aligned nanotube layers is a direct diffusion path for the Li$^+$ ions, resulting in a superior electrochemical performance.[11]

To further increase the capacity and conductivity of the TiO$_2$ nanotubes for their use in LIBs, they have been decorated or coated with other metals and metal oxides, with higher conductivities and capacities, for example, Ag,[17] Cu$_6$Sn$_5$,[18] Fe$_2$O$_3$,[19] SnO,[20] SnO$_2$,[21,22] or ZnO.[23] Another advantage of these composite structures is that due to their hollow tubular architecture they can bear volume variations upon battery cycling without mechanical failure.

Among the various methods that can be used for the coating and decoration of the TiO$_2$ nanotube layers, atomic layer deposition (ALD) has been the only method that creates uniform coatings of the nanotube walls from inside as well as outside, with a precise control of the coating thickness according to the deposition cycles.[24−26] However, although several reports can be found on utilization of the ALD coatings of different materials to modify the electrodes for lithium-ion battery application,[27−33] only one publication reports on the use of ALD to coat an anode prepared from an anodic TiO$_2$ nanotube layer with ZnO.[23]

Usually, passivation layers on the electrode surfaces (solid electrolyte interphase (SEI)) are formed via decomposition of
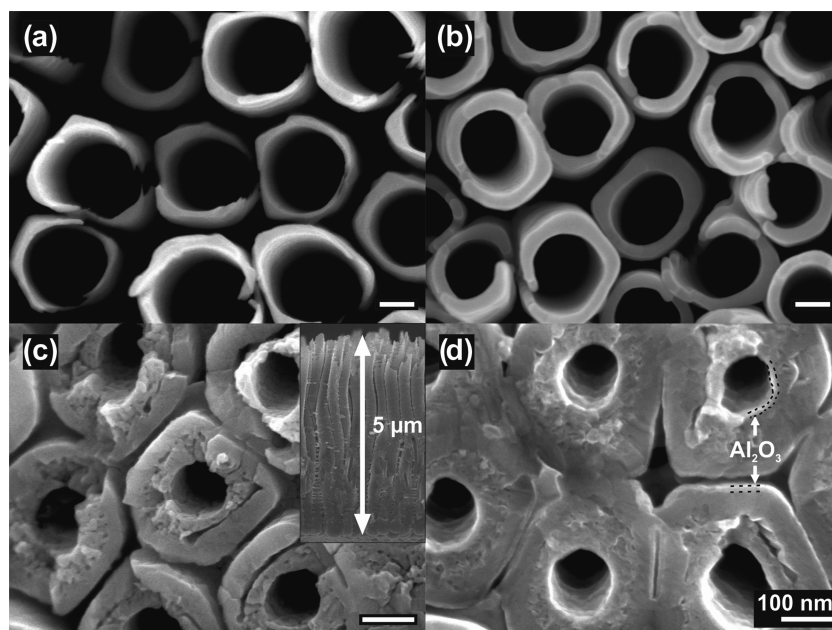
Figure 1. SEM images of the top (a, b) and bottom parts (c, d) of the uncoated TiO_2 nanotube layer (a, c) and 10 nm ALD Al_2O_3-coated TiO_2 nanotube layer (b, d). The inset in (c) shows an illustrative image of the whole TiO_2 nanotube layer, revealing a thickness of ~5 μm.

the electrolyte and are necessary to prevent further electrolyte decomposition that often leads to unsafe operation conditions.[34] However, Li$^+$ ions are consumed for SEI formation, reducing the overall capacity of the electrode. Thin layers of Al_2O_3 can suppress the SEI formation and undesirable side reactions. Several reports demonstrated the beneficial effect of the Al_2O_3 coatings on electrodes prepared from different materials for passivation of the electrode surfaces.[35−43] At the same time, Al_2O_3 acts as a substitute for the SEI layer due to the formation of Li−Al−O in the first few cycles, which is a good ionic conductor, blocking the electron transfer efficiently.[39,40,43]

In this work, for the first time, the vertically aligned TiO_2 nanotube layers prepared by anodization were coated with thin Al_2O_3 layers of different thicknesses by ALD (i.e., 0.2, 1, 2, 5, and 10 nm corresponding to of 2, 9, 18, 46, and 92 ALD cycles, respectively) and examined as potential anodes for LIBs. The results were compared to that of the uncoated TiO_2 nanotube layers.

■ EXPERIMENTAL SECTION

TiO_2 nanotube layers, with a thickness of ~5 μm and a diameter of ~230 nm, were prepared according to the previously published work.[44] In brief, Ti foils (Sigma Aldrich, 0.127 mm thick, 99.7% purity) were degreased in isopropanol and acetone and afterwards anodized in an ethylene glycol-based electrolyte containing 150 mM NH_4F and 10 vol % H_2O at 100 V for 4 h. The electrochemical cell consisted of a high-voltage potentiostat (PGU-200V; Elektroniklabor GmbH) in a two-electrode configuration, with a Pt foil as the counter electrode and Ti foil as the working electrode. After anodization, the nanotube layers were sonicated in isopropanol and dried in air. Before further use, all of the TiO_2 nanotube layers were annealed in a muffle oven at 400 °C to receive a crystalline anatase phase.

The prepared TiO_2 nanotube layers were coated with Al_2O_3 layers of different thicknesses using an ALD tool (thermal ALD, TFS 200, Beneq). Trimethylaluminum (TMA, Strem, elec.

grade, 99.999+%) and deionized water (18 MΩ) were used as aluminum and oxygen precursors, respectively. Under these deposition conditions, one ALD Al_2O_3 growth cycle was defined by the following sequence: TMA pulse (100 ms)−N_2 purge (2 s)−H_2O pulse (100 ms)−N_2 purge (3 s). All processes were carried out at a temperature of 200 °C, using N_2 (99.9999%) as the carrier gas, at a flow rate of 400 sccm. Al_2O_3 coatings of different thicknesses were deposited within the TiO_2 nanotube layers. The number of cycles required for the different Al_2O_3 thicknesses was estimated from the growth per cycle value of the Al_2O_3 process at 200 °C (~1.1 Å/cycle). Thus, ALD processes of 2, 9, 18, 46, and 92 cycles led to nominal Al_2O_3 coating thicknesses of 0.2, 1, 2, 5, and 10 nm, respectively.

The structure and morphology of the TiO_2 nanotube layers were characterized by a field-emission electron microscope (FE-SEM JEOL JSM 7500F). Dimensions of the nanotubes were measured and statistically evaluated using proprietary Nanomeasure software.

The electrochemical performance of the ALD Al_2O_3-coated TiO_2 nanotube layers was studied using Swagelok-type cells. The TiO_2 nanotube layers were assembled with metallic Li (Aldrich) as the counter electrode, with a glass fiber (Whatman) used as a separator. The electrolyte consisted of a solution of 1 M $LiPF_6$ in ethylene carbonate (EC)/diethyl carbonate (DEC) (1:1, in w/w) (Sigma Aldrich). The cells were assembled in an argon-filled glovebox (MBraun, Germany), with <0.5 ppm H_2O and <0.5 ppm O_2 atmosphere. Galvanostatic tests were carried out using a VMP3 potentiostat (Bio Logic, France). The cells were cycled at 1C (~1 h charge/discharge) in a potential window of 1−3 V. The current was applied considering the mass of the TiO_2 nanotube layers and was calculated considering a density of 4.23 g/cm^3 and porosity of 76%. The porosity calculation is based on the amount of the TiO_2 nanotubes per cm^2. The volume occupied by the TiO_2 nanotubes was calculated by subtracting the inner tube area from outer tube area.
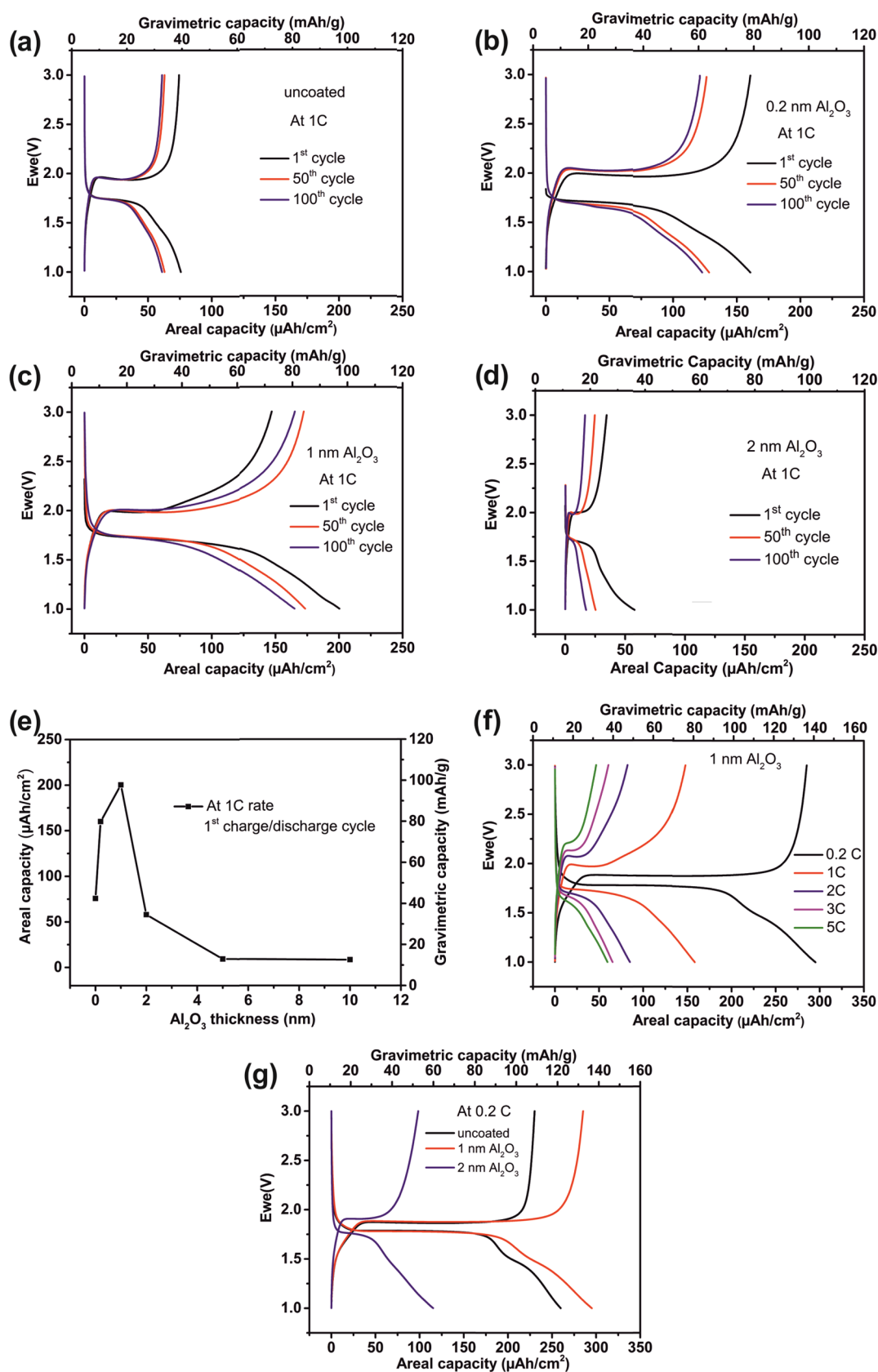
Figure 2. Galvanostatic cycling at 1C rate of the (a) uncoated (0 cycles), (b) 0.2 nm (2 cycles), (c) 1 nm (9 cycles), and (d) 2 nm (18 cycles) ALD Al$_2$O$_3$-coated TiO$_2$ nanotube layers, (e) the discharge capacity of the first charge/discharge cycle of the TiO$_2$ nanotube layers coated with Al$_2$O$_3$ of different thicknesses at 1C rate, (f) galvanostatic discharge/charge curves of the first reversible cycle of the 1 nm Al$_2$O$_3$-coated TiO$_2$ nanotube layer at different C rates, and (g) galvanostatic discharge/charge curves of the first reversible cycle of the uncoated, and the 1 and 2 nm ALD Al$_2$O$_3$-coated TiO$_2$ nanotube layer at C/5.

The chronoamperometric (CA) tests were conducted in a three-electrode Swagelok cell. The uncoated and the 1 and 2 nm ALD Al_2O_3-coated TiO_2 nanotube layer electrodes were assembled against one Li foil serving as a counter electrode and another Li foil as a reference electrode. Two separators were placed between each electrode soaked in a solution of 1 M $LiPF_6$ in EC/DEC (1:1, in w/w) obtained from Sigma Aldrich. The CA tests were performed by applying a constant potential of 1.7 V for 80 s using a VMP3 potentiostat−galvanostat (Bio Logic).

For electrochemical impedance spectroscopy (EIS) measurements, the nanotube layers were assembled in a three-electrode system, with separate Li foils as the reference and counter electrodes, using Whatman paper as the separator. EC/DEC with 1 M $LiPF_6$ was used as the electrolyte. The cells were kept for 24 h at open circuit potential (OCP) to get stabilized. The AC impedance measurements were carried out using a VMP3 Biologic Potentiostat at OCP in a frequency range of 100 kHz to 10 mHz at amplitude of 10 mV. The obtained spectra were fitted by "Z-fit" in the EC-Lab software (Bio Logic).

■ RESULTS AND DISCUSSION

Figure 1 shows SEM images of the top (a, b) and bottom parts (c, d) of the uncoated TiO_2 nanotube layer and the 10 nm Al_2O_3-coated TiO_2 nanotube layer. As can be seen, the wall thickness on top of the nanotube layers increased from the uncoated to 10 nm ALD Al_2O_3-coated TiO_2 nanotube layers. At the bottom parts, thin layers of Al_2O_3 could be observed on the inside as well as outside of the nanotube walls. The thin layers were visible due to the different mass contrasts between TiO_2 and Al_2O_3. In line with our previous work, the ALD Al_2O_3 coatings on the TiO_2 nanotube layers were very uniform and homogenous.[26]

It has to be noted that the double-walled structure that can be seen at the bottom parts of both the uncoated and coated nanotube layers is an intrinsic feature of the TiO_2 nanotube layers prepared in ethylene glycol-based electrolytes and is well known from the literature.[45]

Figure 2a−d shows the charge/discharge profiles obtained by chronopotentiometry in the potential range of 1.0−3.0 V for the uncoated TiO_2 nanotubes (taken as reference), 0.2 nm Al_2O_3, 1 nm Al_2O_3, and 2 nm ALD Al_2O_3-coated TiO_2 nanotube layers recorded at 1C. In all of the cases, the presence of two plateaus is attributed to the reversible insertion of Li^+ into crystalline anatase TiO_2. In the discharge profile, the plateau at ~1.75 V corresponds to the accommodation of Li^+, according to a reduction reaction. In the charge profile, the plateau at ~1.95 V was induced by the extraction of Li^+, according to an oxidation reaction. The reversible insertion reaction of Li^+ in anatase TiO_2 is given by eq 1[1]

$$TiO_2 + xLi^+ + xe^- \leftrightarrow Li_xTiO_2 \text{ for } 0 \leq x \leq 0.5 \qquad (1)$$

As can be seen in Figure 2a−d, the presence of Al_2O_3 coating clearly had a strong influence on the electrochemical performance of the TiO_2 nanotube electrodes. Indeed, the areal and gravimetric capacities grew with increasing Al_2O_3 thickness until a maximum value for the 1 nm Al_2O_3-coated TiO_2 nanotube layers and then decreased for the TiO_2 nanotube layers with thicker coatings. The gravimetric capacities were calculated on the basis of an estimated porosity of 76%. It must be noted that the porosity of the nanotube layers is just an estimated value and therefore the gravimetric capacities are not

as accurate as the areal capacities. The theoretical capacity of TiO_2 is 336 mAh/g for 1 mol of Li-ion insertion. For the fully reversible reaction, TiO_2 inserts a maximum of 0.5 mol Li ions, giving a theoretical capacity of 168 mAh/g.[1] Thus, the theoretical capacity is not reached for 1 nm coatings, according to our porosity calculation. However, the calculated gravimetric capacity for the nanotube layers with 1 nm coating was 149 mAh/g for the first cycle at a C rate of C/5 (Figure 2f,g), which is very close to the theoretical value of 168 mAh/g, especially taking the above mentioned accuracy into account.

Figure 2e shows dependence of the first discharge capacity delivered by the TiO_2 nanotube layers coated by Al_2O_3, using various coating thicknesses. After being coated with 1 nm Al_2O_3, the areal capacity was more than 2 times higher compared to that of the reference (~200 vs ~75 $\mu Ah/cm^2$, respectively), whereas for thicker Al_2O_3 coatings, the areal capacity decreased significantly. More remarkably, after the charge/discharge tests, the capacity remained almost 3 times higher than that for the reference (~164 vs ~60 $\mu Ah/cm^2$, respectively).

Reasons for the enhancement of capacity on the Al_2O_3-coated TiO_2 nanotube layers are at least 2-fold. At first, an inhibition of the significant volume changes of the TiO_2 nanotubes during Li insertion due to an improved mechanical stability should be considered. An improved mechanical and chemical stability of the ALD Al_2O_3-coated TiO_2 nanotube arrays was recently reported by the Macak group,[46] showing that already thin Al_2O_3 coatings of 1 nm have a beneficial effect. Moreover, it was reported that an addition of Al_2O_3 can stabilize the mesoporous anatase TiO_2 structures upon Li insertion.[47] However, SEM analyses of the electrodes was carried out after 100 charge/discharge cycles, presented in Figure 2. All of the nanotube layers preserved their architecture (see Figure S1) without any noticeable change or damage.

The second reason for the enhanced capacity is a better diffusion of the Li^+ ions within the Al_2O_3-coated TiO_2 nanotube layers, which might be explained by changes in the Al_2O_3 layer upon galvanostatic experiments. Xiao et al.[41] found that the structure of the ultrathin Al_2O_3 changes to Al_2O_3/AlF_3 during cycling, providing a better Li^+-ion conductivity and formation of $LiAlO_2$ on the surface that can promote Li insertion by reducing the associated energy barrier.

However, on the basis of Figure 2, a suppression of the SEI layer due to Al_2O_3 coatings can be excluded, even though Al_2O_3 coatings are typically discussed in the literature[39,40,43] as inhibitors of SEI formation. It is also known that on the TiO_2 anodes only very thin SEI layers are formed when electrochemical cycling experiments are performed at potentials higher than 1 V.[2,11,48] Indeed, from Figure 2 it is clear that the capacity loss during the first charge/discharge cycle (when SEI typically forms) was very low for the uncoated TiO_2 nanotube layer, suggesting that only a very thin SEI layer was formed. In contrast, the capacity loss during the first charge/discharge cycle was much more pronounced for the Al_2O_3-coated TiO_2 nanotube layers. This high irreversible capacity of the ALD Al_2O_3-coated TiO_2 nanotube layers might be caused by Li-containing Al_2O_3 phase formation.[39] It is believed that the insulating Al_2O_3 layers cause a potential drop and also slow down Li diffusion during the first cycle. Thereafter, Al_2O_3 reacts with the electrolyte and forms AlF_3, which facilitates the charge transfer.[39] It was also suggested that lithiation of the Al_2O_3 coating layer proceeds until a thermodynamically stable phase is reached (corresponding to $Li_{3.4}Al_2O_3$).[49] The extra Li^+ ions

then overflow into the electrode passing through the coating layer. If the Al_2O_3 coating layer is too thick, a longer time would be needed until the thermodynamically stable phase is reached.[49] This explains that thicker Al_2O_3 coatings blocked Li diffusion into TiO_2 and therefore the areal capacity decreased for the thicker Al_2O_3 coatings within the TiO_2 nanotube layers, as can be seen in Figure 2e. Furthermore, a higher amount of Li^+ from the electrolyte is needed to build a thermodynamically stable phase $Li_{3.4}Al_2O_3$ for the thicker Al_2O_3 layers, reducing the charge/discharge capacities.

Additionally, calculations of the diffusion coefficients using chronoamperometry and the Cottrell equation were carried out after cycling the cell for three cycles at 1C rate to facilitate formation of the Li−Al−O phase (see Figure S2). The diffusion coefficients calculated for the uncoated (0 cycles ALD) and 1 nm (9 cycles) ALD Al_2O_3-coated TiO_2 nanotube layers were 1 × 10^{-16} and 1.44 × 10^{-16} cm^2 s^{-1}, respectively, which shows the positive influence of Al_2O_3 on Li^+ diffusion. For the 2 nm (18 cycles) ALD Al_2O_3-coated TiO_2 nanotube layers, the diffusion coefficient was estimated to be 9 × 10^{-17} cm^2 s^{-1}, suggesting that at a higher Al_2O_3 thickness Li^+ diffusion is hindered.

Lindstrom et al.[50] have reported an Li^+ diffusion coefficient of 1 × 10^{-17} cm^2 s^{-1} for nanoporous anatase TiO_2 using chronoamperometry. Apart from the positive influence of the thin Al_2O_3 coating on the TiO_2 nanotubes shown for our samples, the higher Li^+ diffusion also indicates that one-dimensional nanomaterials (like the vertical aligned nanotubes) could help promote better charge diffusion compared with nanoporous films.

These results are also in agreement with findings reported in the literature. Lipson et al.[43] observed for an ALD Al_2O_3-coated MnO electrode that Li^+ was unable to diffuse through the thick Al_2O_3 films and thus the thick ALD Al_2O_3 films blocked the electrode surface. Ultrathin Al_2O_3 films (9 Å thick), however, inhibited SEI formation without blocking the electrode surface.

Considering the superior performance for the 1 nm Al_2O_3-coated TiO_2 nanotube layer at 1C, cycling tests at faster kinetics have been explored to study the rate capability of this coating in more detail. As shown in Figure 2f, the discharge capacities of the first reversible cycle were ~295, ~158, ~84, ~65, and ~59 $\mu Ah/cm^2$ for C/5, 1C, 2C, 3C, and 5C, respectively. As expected, the areal capacity decreased with an increased C rate due to the higher applied current density. Figure 2g shows the galvanostatic discharge/charge curves of the first reversible cycle of the uncoated and the 1 and 2 nm ALD Al_2O_3-coated TiO_2 nanotube layer at 0.2C. As can be seen, the theoretical gravimetric capacity was just reached in the case of the 1 nm ALD Al_2O_3-coated TiO_2 nanotube layer, taking accuracy of the porosity calculation into account. It can be pointed out that these high capacity values obtained for the 1 nm ALD Al_2O_3-coated TiO_2 nanotube layer were only obtained by the uncoated TiO_2 nanotube layers at very slow kinetics (C/10).

The coulombic efficiencies (CEs) for the first charge/discharge cycles for the uncoated and 1 nm ALD Al_2O_3-coated TiO_2 nanotube layers are given in Table 1. As expected, the CE for the uncoated TiO_2 nanotube layer was very high from the first charge/discharge cycle. The CE of the 1 nm ALD Al_2O_3-coated TiO_2 nanotube layer, however, is comparably lower during the first 10 cycles. This is probably due to the formation of the Li−Al−O phase during the first charge/discharge cycles.

Figure 3a depicts the discharge capacities of the uncoated TiO_2 nanotube layer and the 1 nm Al_2O_3-coated TiO_2 nanotube layer for the 100 charge/discharge cycles at 1C.

Table 1. CEs for the First Charge/Discharge Cycles for the Uncoated and 1 nm ALD Al_2O_3-Coated TiO_2 Nanotube Layers

charge/discharge cycle no.	CE of the uncoated TiO_2 nanotube layer (%)	CE of the 1 nm ALD Al_2O_3-coated TiO_2 nanotube layer (%)
1	92.2	73.2
2	98.85	93.03
3	98.35	93.80
5	99.05	95.67
10	99.13	97.54

After an initial decrease of the capacity during the initial discharge cycle, more than 2 times higher capacity was attained for the 1 nm Al_2O_3-coated TiO_2 nanotube layer compared to that of the reference. However, a very slight decrease of the discharge capacity could be seen for the uncoated nanotube layer, whereas for the 1 nm Al_2O_3-coated TiO_2 nanotube layer, an increase of the discharge capacity was clearly visible during the first cycles. This increase might be explained with an increase in conductivity of the Al_2O_3 coating during the electrochemical cycling, as explained above. All in all, the 2-fold difference was preserved even after extensive cycling.

EIS measurements were performed to further elucidate the effect of the Al_2O_3 coatings on TiO_2 nanotube layers. Figure 3b shows the overlaid impedance spectra of both samples and their fittings at OCP. The figure demonstrates the excellent agreement between the experimental and fit data. The equivalent circuit for the EIS spectra of the uncoated TiO_2 nanotube layer is represented by $[R_e + R_{CT}/Q_{CT} + Q]$, shown in Figure 4a, where R represents resistors and Q, constant phase elements (CPEs). R_e represents essentially the resistance of the electrolyte. The depressed semicircle at the medium frequency and the sloped line at low frequencies represent the charge-transfer impedance (R_{CT}/Q_{CT}) of the lithium intercalation process and the capacitive effect (Q), respectively. From the fit data of the EIS spectra, R_{CT} for the uncoated TiO_2 nanotube layer was 692.2 Ω.

The EIS spectrum for the Al_2O_3-coated TiO_2 nanotube layer consists of two semicircles. The first depressed semicircle at high frequency is attributed to the impedance due to the Al_2O_3 coating on the nanotube layer[51] and the second semicircle in the medium frequency range to the impedance due to the charge transfer resistance. The equivalent circuit shown in Figure 4b for the 1 nm Al_2O_3-coated TiO_2 nanotube layer is $[R_e + R_{Al_2O_3}/Q_{Al_2O_3} + R_{CT}/Q_{CT} + Q]$. From the fit data, $R_{Al_2O_3}$ and R_{CT} were calculated to be 56.07 and 289.1 Ω, respectively. The exponent for the last CPE was 0.8 for both samples, which suggests largely a capacitive effect. The lower R_{CT} for the 1 nm ALD Al_2O_3-coated TiO_2 nanotube layer revealed a positive influence of the Al_2O_3 coating in enhancing the electronic conductivity of the TiO_2 nanotube layer.

Another advantage of the Al_2O_3 coating is that it can also prevent the electrolyte side reactions with TiO_2 during the charge/discharge process, thereby suppressing any passivation layer on the surface of the TiO_2 nanotube layer.

■ CONCLUSIONS

In summary, it was demonstrated that the ALD coating of the TiO_2 nanotube layers, with thin layers (≤1 nm) of Al_2O_3, have a beneficial effect on the areal capacity and cycling behavior of the TiO_2 nanotube layers. This is due to an increased
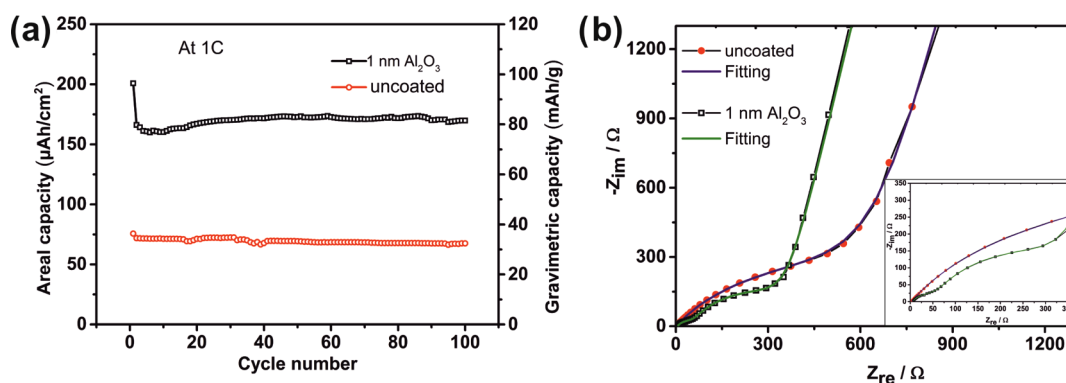
Figure 3. Discharge capacity as a function of the discharge cycle number of the cells at 1C rate (a) and Nyquist plots (at OCP vs Li/Li$^+$) (b) for the uncoated and 1 nm ALD Al$_2$O$_3$-coated TiO$_2$ nanotube layers. The inset in (b) shows a higher magnification of the first semicycle.
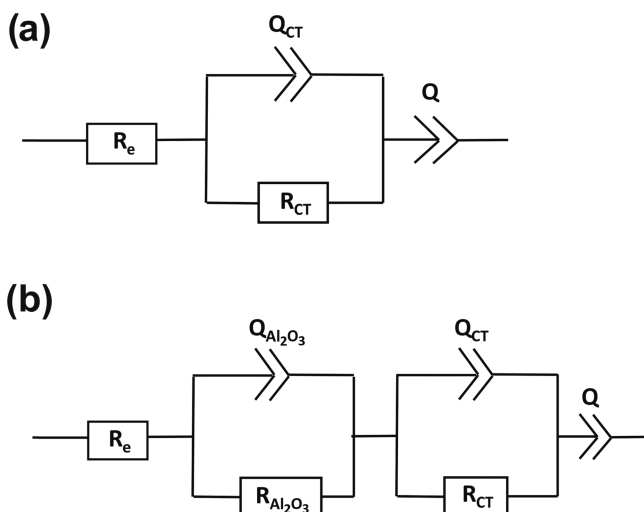

Figure 4. Equivalent circuits for the EIS plots of the (a) uncoated and (b) 1 nm ALD Al$_2$O$_3$-coated TiO$_2$ nanotube layers.

mechanical stability of the nanotube layers upon Al$_2$O$_3$ coating and a better diffusion of the Li$^+$ ions within the Al$_2$O$_3$-coated TiO$_2$ nanotube layers. On the other hand, Al$_2$O$_3$ coatings with thickness >2 nm show a reduced capacity. The approach presented in this work is important for future applications of the TiO$_2$ nanotube layers, where a thin and highly conformal coating of the secondary material can significantly enhance the performance of the TiO$_2$ nanotube layers and explore these composite nanotube layers for new applications, previously unfeasible for the uncoated (bare) TiO$_2$ nanotube layers.

ASSOCIATED CONTENT

Ⓢ Supporting Information

The Supporting Information is available free of charge on the ACS Publications website at DOI: 10.1021/acsomega.7b00463.

Postcycling SEM images; chronoamperometric plots (PDF)

AUTHOR INFORMATION

Corresponding Authors
*E-mail: thierry.djenizian@mines-stetienne.fr (T.D.).
*E-mail: jan.macak@upce.cz (J.M.M.).

ORCID Ⓞ
Jan M. Macak: 0000-0001-7091-3022

Notes

The authors declare no competing financial interest.

REFERENCES

(1) Ortiz, G. F.; Hanzu, I.; Djenizian, T.; Lavela, P.; Tirado, J. L.; Knauth, P. Alternative Li-Ion Battery Electrode Based on Self-Organized Titania Nanotubes. *Chem. Mater.* **2009**, *21*, 63−67.

(2) Djenizian, T.; Hanzu, I.; Knauth, P. Nanostructured Negative Electrodes Based on Titania for Li-Ion Microbatteries. *J. Mater. Chem.* **2011**, *21*, 9925−9937.

(3) González, J. R.; Alcántara, R.; Nacimiento, F.; Ortiz, G. F.; Tirado, J. L.; Zhecheva, E.; Stoyanova, R. Long-Length Titania Nanotubes Obtained by High-Voltage Anodization and High-Intensity Ultrasonication for Superior Capacity Electrode. *J. Phys. Chem. C* **2012**, *116*, 20182−20190.

(4) Lee, K.; Mazare, A.; Schmuki, P. One-Dimensional Titanium Dioxide Nanomaterials: Nanotubes. *Chem. Rev.* **2014**, *114*, 9385−9454.

(5) Liu, H.; Bi, Z.; Sun, X.-G.; Unocic, R. R.; Paranthaman, M. P.; Dai, S.; Brown, G. M. Mesoporous TiO$_2$−B Microspheres with Superior Rate Performance for Lithium Ion Batteries. *Adv. Mater.* **2011**, *23*, 3450−3454.

(6) Armstrong, A. R.; Armstrong, G.; Canales, J.; Bruce, P. G. TiO$_2$-B Nanowires. *Angew. Chem., Int. Ed.* **2004**, *43*, 2286−2288.

(7) Armstrong, A. R.; Armstrong, G.; Canales, J.; García, R.; Bruce, P. G. Lithium-Ion Intercalation into TiO$_2$-B Nanowires. *Adv. Mater.* **2005**, *17*, 862−865.

(8) Ren, Y.; Liu, Z.; Pourpoint, F.; Armstrong, A. R.; Grey, C. G.; Bruce, P. G. Nanoparticulate TiO$_2$(B): An Anode for Lithium-Ion Batteries. *Angew. Chem., Int. Ed.* **2012**, *51*, 2164−2167.

(9) Yang, M.-C.; Lee, Y. Y.; Xu, B.; Powers, K.; Meng, Y. S. TiO$_2$ Flakes as Anode Materials for Li-Ion-Batteries. *J. Power Sources* **2012**, *207*, 166−172.

(10) Panda, S. K.; Lee, S.; Yoon, W.-S.; Shin, H. Reversible Phase Transformation of Titania (Anatase) Nanotubes upon Electrochemical Lithium-Intercalation Observed by Ex Situ Transmission Electron Microscopy. *J. Power Sources* **2014**, *249*, 59−65.

(11) Han, H.; Song, T.; Lee, E.-K.; Devadoss, A.; Jeon, Y.; Ha, J.; Chung, Y.-C.; Choi, Y.-M.; Jung, Y.-G.; Paik, U. Dominant Factors

Governing the Rate Capability of a TiO2 Nanotube Anode for High Power Lithium Ion Batteries. *ACS Nano* **2012**, *6*, 8308−8315.

(12) Ellis, B. L.; Knauth, P.; Djenizian, T. Three-Dimensional Self-Supported Metal Oxides for Advanced Energy Storage. *Adv. Mater.* **2014**, *26*, 3368−3397.

(13) Salian, G. D.; Lebouin, C.; Demoulin, A.; Lepikhin, M. S.; Maria, S.; Galyyeva, A. K.; Kurbatov, A. P.; Djenizian, T. Electrodeposition of Polymer Electrolyte in Nanostructured Electrodes for Enhanced Electrochemical Performance of Thin-Film Li-Ion Microbatteries. *J. Power Sources* **2017**, *340*, 242−246.

(14) Plylahan, N.; Letiche, M.; Barr, M.; Ellis, B.; Maria, S.; Phan, T. N. T.; Bloch, E.; Knauth, P.; Djenizian, T. High Energy and Power Density TiO2 Nanotube Electrodes for Single and Complete Lithium-Ion Batteries. *J. Power Sources* **2015**, *273*, 1182−1188.

(15) Plylahan, N.; Letiche, M.; Barr, M.; Djenizian, T. All-Solid-State Li-Ion Batteries Based on Self-Supported Titania Nanotubes. *Electrochem. Commun.* **2014**, *43*, 121−124.

(16) Macak, J. M.; Tsuchiya, H.; Ghicov, A.; Yasuda, K.; Hahn, R.; Bauer, S.; Schmuki, P. TiO2 Nanotubes: Self-Organized Electrochemical Formation, Properties and Applications. *Curr. Opin. Solid State Mater. Sci.* **2007**, *11*, 3−18.

(17) Fang, D.; Huang, K.; Liu, S.; Li, Z. Electrochemical Properties of Ordered TiO2 Nanotube Loaded with Ag Nano-Particles for Lithium Anode Material. *J. Alloys Compd.* **2008**, *464*, L5−L9.

(18) Xue, L.; Wei, Z.; Li, R.; Liu, J.; Huang, T.; Yu, A. Design and Synthesis of Cu6Sn5-Coated TiO2 Nanotube Arrays as Anode Material for Lithium Ion Batteries. *J. Mater. Chem.* **2011**, *21*, 3216−3220.

(19) Ortiz, G. F.; Hanzu, I.; Lavela, P.; Tirado, J. L.; Knauth, P.; Djenizian, T. A Novel Architectured Negative Electrode Based on Titania Nanotube and Iron Oxide Nanowire Composites for Li-Ion Microbatteries. *J. Mater. Chem.* **2010**, *20*, 4041−4046.

(20) Ortiz, G. F.; Hanzu, I.; Lavela, P.; Knauth, P.; Tirado, J. L.; Djenizian, T. Nanoarchitectured TiO2/SnO: A Future Negative Electrode for High Power Density Li-Ion Microbatteries? *Chem. Mater.* **2010**, *22*, 1926−1932.

(21) Du, G.; Guo, Z.; Zhang, P.; Li, Y.; Chen, M.; Wexler, D.; Liu, H. SnO2 Nanocrystals on Self-Organized TiO2 Nanotube Array as Three-Dimensional Electrode for Lithium Ion Microbatteries. *J. Mater. Chem.* **2010**, *20*, 5689−5694.

(22) Wu, X.; Zhang, S.; Wang, L.; Du, Z.; Fang, H.; Ling, Y.; Huang, Z. Coaxial SnO2@TiO2 Nanotube Hybrids: From Robust Assembly Strategies to Potential Application in Li+ Storage. *J. Mater. Chem.* **2012**, *22*, 11151−11158.

(23) Li, R.; Xie, Z.; Lu, H.; Zhang, D. W.; Yu, A. Fabrication of ZnO@TiO2 Core-Shell Nanotube Arrays as Three-Dimensional Anode Material for Lithium Ion Batteries. *Int. J. Electrochem. Sci.* **2013**, *8*, 11118−11124.

(24) Tupala, J.; Kemell, M.; Härkönen, E.; Ritala, M.; Leskelä, M. Preparation of Regularly Structured Nanotubular TiO2 Thin Films on ITO and Their Modification with Thin ALD-Grown Layers. *Nanotechnology* **2012**, *23*, No. 125707.

(25) Macak, J. M.; Prikryl, J.; Sopha, H.; Strizik, L. Antireflection In2O3 Coatings of Self-Organized TiO2 Nanotube Layers Prepared by Atomic Layer Deposition. *Phys. Status Solidi RRL* **2015**, *9*, 516−520.

(26) Zazpe, R.; Knaut, M.; Sopha, H.; Hromadko, L.; Albert, M.; Prikryl, J.; Gärtnerová, V.; Bartha, J. W.; Macak, J. M. Atomic Layer Deposition for Coating of High Aspect Ratio TiO2 Nanotube Layers. *Langmuir* **2016**, *32*, 10551−10558.

(27) Cheah, S. K.; Perre, E.; Rooth, M.; Fondell, M.; Hårsta, A.; Nyholm, L.; Boman, M.; Gustafsson, T.; Lu, J.; Simon, P.; Edström, K. Self-Supported Three-Dimensional Nanoelectrodes for Microbattery Applications. *Nano Lett.* **2009**, *9*, 3230−3233.

(28) Scott, I. D.; Jung, Y. S.; Cavanagh, A. S.; Yan, Y.; Dillon, A. C.; George, S. M.; Lee, S.-H. Ultrathin Coatings on Nano-LiCoO2 for Li-Ion Vehicular Applications. *Nano Lett.* **2011**, *11*, 414−418.

(29) Memarzadeh Lotfabad, E.; Kalisvaart, P.; Cui, K.; Kohandehghan, A.; Kupsta, M.; Olsen, B.; Mitlin, D. ALD TiO2 Coated Silicon Nanowires for Lithium Ion Battery Anodes With Enhanced Cycling Stability and Coulombic Efficiency. *Phys. Chem. Chem. Phys.* **2013**, *15*, 13646−13657.

(30) Lotfabad, E. M.; Kalisvaart, P.; Kohandehghan, A.; Cui, K.; Kupsta, M.; Olsen, B.; Farbod, B.; Mitlin, D. Si Nanotubes ALD Coated With TiO2, TiN or Al2O3 As High Performance Lithium Ion Battery Anodes. *J. Mater. Chem. A* **2014**, *2*, 2504−2516.

(31) Zhang, H.; Ren, W.; Cheng, C. Three-Dimensional SnO2@TiO2 Double-Shell Nanotubes on Carbon Cloth as a Flexible Anode for Lithium-Ion Batteries. *Nanotechnology* **2015**, *26*, No. 274002.

(32) Lv, X.; Deng, J.; Sun, X. Cumulative Effect of Fe2O3 on TiO2 Nanotubes via Atomic Layer Deposition with Enhanced Lithium Ion Storage Performance. *Appl. Surf. Sci.* **2016**, *369*, 314−319.

(33) Zhong, Y.; Ma, Y.; Guo, Q.; Liu, J.; Wang, Y.; Yang, M.; Xia, H. Controllable Synthesis of TiO2@Fe2O3 Core-Shell Nanotube Arrays with Double-Wall Coating as Superb Lithium-Ion Battery Anodes. *Sci. Rep.* **2017**, *7*, No. 40927.

(34) Vetter, J.; Novak, P.; Wagner, M. R.; Veit, C.; Moller, K. C.; Besenhard, J. O.; Winter, M.; Wohlfahrt-Mehrens, M.; Vogler, C.; Hammouche, A. Ageing Mechanisms in Lithium-Ion Batteries. *J. Power Sources* **2005**, *147*, 269−281.

(35) Jung, Y. S.; Cavanagh, A. S.; Riley, L. A.; Kang, S.-H.; Dillon, A. C.; Groner, M. D.; George, S. M.; Lee, S.-H. Ultrathin Direct Atomic Layer Deposition on Composite Electrodes for Highly Durable and Safe Li-Ion Batteries. *Adv. Mater.* **2010**, *22*, 2172−2176.

(36) Liu, Y.; Hudak, N. S.; Huber, D. L.; Limmer, S. J.; Sullivan, J. P.; Huang, J. Y. In Situ Transmission Electron Microscopy Observation of Pulverization of Aluminum Nanowires and Evolution of the Thin Surface Al2O3 Layers during Lithiation-Delithiation Cycles. *Nano Lett.* **2011**, *11*, 4188−4194.

(37) Leung, K.; Qi, Y.; Zavadil, K. R.; Jung, Y. S.; Dillon, A. C.; Cavanagh, A. S.; Lee, S.-H.; George, S. M. Using Atomic Layer Deposition to Hinder Solvent Decomposition in Lithium Ion Batteries: First-Principles Modeling and Experimental Studies. *J. Am. Chem. Soc.* **2011**, *133*, 14741−14754.

(38) Lahiri, I.; Oh, S.-M.; Hwang, J. Y.; Chiwon Kang, C.; Choi, M.; Jeon, H.; Banerjee, R.; Sun, Y.-K.; Choi, W. Ultrathin Alumina-Coated Carbon Nanotubes as an Anode for High Capacity Li-Ion Batteries. *J. Mater. Chem.* **2011**, *21*, 13621−13626.

(39) Ahn, D.; Xiao, X. Extended Lithium Titanate Cycling Potential Window with Near Zero Capacity Loss. *Electrochem. Commun.* **2011**, *13*, 796−799.

(40) Nguyen, H. T.; Zamfir, M. R.; Duong, L. D.; Lee, Y. H.; Paolo Bondavallic, P.; Pribat, D. Alumina-Coated Silicon-Based Nanowire Arrays for High Quality Li-Ion Battery Anodes. *J. Mater. Chem.* **2012**, *22*, 24618−24626.

(41) Xiao, X.; Peng Lu, P.; Ahn, D. Ultrathin Multifunctional Oxide Coatings for Lithium Ion Batteries. *Adv. Mater.* **2011**, *23*, 3911−3915.

(42) He, Y.; Yu, X.; Wang, Y.; Li, H.; Huang, X. Alumina-Coated Patterned Amorphous Silicon as the Anode for a Lithium-Ion Battery with High Coulombic Efficiency. *Adv. Mater.* **2011**, *23*, 4938−4941.

(43) Lipson, A. L.; Puntambekar, K.; Comstock, D. J.; Meng, X.; Geier, M. L.; Elam, J. W.; Hersam, M. C. Nanoscale Investigation of Solid Electrolyte Interphase Inhibition on Li-Ion Battery MnO Electrodes via Atomic Layer Deposition of Al2O3. *Chem. Mater.* **2014**, *26*, 935−940.

(44) Das, S.; Sopha, H.; Krbal, M.; Zazpe, R.; Podzemna, V.; Prikryl, J.; Macak, J. M. Electrochemical Infilling of CuInSe2 within TiO2 Layers and Their Photoelectrochemical Studies. *ChemElectroChem* **2017**, *4*, 495−499.

(45) Albu, S. P.; Ghicov, A.; Aldabergenova, S.; Drechsel, P.; LeClere, D.; Thompson, G. E.; Macak, J. M.; Schmuki, P. Formation of Double-Walled TiO2 Nanotubes and Robust Anatase Membranes. *Adv. Mater.* **2008**, *20*, 4135−4139.

(46) Zazpe, R.; Prikryl, J.; Gärtnerova, V.; Nechvilova, K.; Benes, L.; Strizik, L.; Jäger, A.; Bosund, M.; Sopha, H.; Macak, J. M. ALD Al2O3 Coatings Significantly Improve Thermal, Chemical and Mechanical Stability of Anodic TiO2 Nanotube Layers. *Langmuir* **2017**, *33*, 3208−3216.

(47) Attia, A.; Zukalova, M.; Rathouský, J.; Zukal, A.; Kavan, L. Mesoporous electrode material from alumina-stabilized anatase TiO$_2$ for lithium ion batteries. *J. Solid State Electrochem.* **2005**, *9*, 138−145.

(48) Deng, D.; Kim, M. G.; Lee, J. Y.; Cho, J. Green Energy Storage Materials: Nanostructured TiO$_2$ and Sn-Based Anodes for Lithium-Ion Batteries. *Energy Environ. Sci.* **2009**, *2*, 818−837.

(49) Jung, S. C.; Han, Y.-K. How Do Li Atoms Pass through the Al$_2$O$_3$ Coating Layer during Lithiation in Li-ion Batteries? *J. Phys. Chem. Lett.* **2013**, *4*, 2681−2685.

(50) Lindstrom, H.; Sodergren, S.; Solbrand, A.; Rensmo, H.; Hjelm, J.; Hagfeldt, A.; Lindquist, S. E. Li$^+$ Ion Insertion in TiO$_2$ (Anatase). 1. Chronoamperometry on CVD Films and Nanoporous Films. *J. Phys. Chem. B* **1997**, *101*, 7710−7716.

(51) Fang, D.; Li, L.; Xu, W.; Zheng, H.; Xu, J.; Jiang, M.; Liu, R.; Jiang, X.; Luo, Z.; Xiong, C.; Wang, Q. High Capacity Lithium Ion Battery Anodes Using Sn Nanowires Encapsulated Al$_2$O$_3$ Tubes in Carbon Matrix. *Adv. Mater. Interfaces* **2016**, *3*, No. 1500491.